Perturbations of the Distal Heme Pocket in Human Myoglobin Mutants Probed by Infrared Spectroscopy of Bound CO: Correlation with Ligand Binding Kinetics

Sriram Balasubramanian, David G. Lambright, Steven G. Boxer

Proceedings of the National Academy of Sciences of the United States of America, Volume 90, Issue 10 (May 15, 1993), 4718-4722.

Proc. Natl. Acad. Sci. USA
Vol. 90, pp. 4718–4722, May 1993
Biochemistry

Perturbations of the distal heme pocket in human myoglobin mutants probed by infrared spectroscopy of bound CO: Correlation with ligand binding kinetics

SRIRAM BALASUBRAMANIAN, DAVID G. LAMBRIGHT, AND STEVEN G. BOXER

Department of Chemistry, Stanford University, Stanford, CA 94305-5080

Communicated by John I. Brauman, January 25, 1993 (received for review October 14, 1992)

ABSTRACT **The infrared spectra of CO bound to human myoglobin and myoglobin mutants at positions His-64, Val-68, Asp-60, and Lys-45 on the distal side have been measured between 100 and 300 K. Large differences are observed with mutations at His-64 and Val-68 as well as with temperature and pH. Although distal His-64 is found to affect CO bonding, Val-68 also plays a major role. The variations are analyzed qualitatively in terms of a simple model involving steric interaction between the bound CO and the distal residues. A strong correlation is found between the final barrier height to CO recombination and the CO stretch frequency: as compared to wild type, the barrier is smaller in those mutants that have a higher CO stretch frequency (ν_{CO}) and vice versa. Possible reasons for this correlation are discussed. It is emphasized that the temperature and pH dependence of both the kinetics and the infrared spectra must be measured to obtain a consistent picture.**

It is generally accepted that the distal His residue at position 64 (Fig. 1) plays a pivotal role in determining the bonding of diatomic ligands to the heme iron in myoglobin (Mb) and hemoglobin (Hb). Comparisons of the binding constants and structures for CO bound to model compounds and the native proteins have led to the general hypothesis that "the linear binding of CO is prevented mainly by the steric hindrance of the distal histidine" (3). Examination of the structure of the heme pocket on the distal side (Fig. 1) indicates that other nearby residues may also affect the accessibility and orientation of bound ligands. Furthermore, in contrast to model compounds that focus on at most one or two critical elements of the heme environment, the residues lining the heme pocket are densely packed, and steric and electrostatic interactions among many amino acid residues may be as important as a specific interaction between the bound ligand and any one residue.

One of the best approaches for studying the precise bonding and structure of the bound ligand is infrared (IR) spectroscopy (4, 5). Two basic pieces of information are obtained from the vibrational spectrum: the CO stretching frequency ν_{CO}, which is an indirect measure of the Fe–CO bond strength, and the angle of the CO relative to the heme normal (see Fig. 1), which reflects the steric interaction between the bound CO and neighboring residues. These observables are themselves correlated because the degree of bending of the CO affects the Fe–CO bond strength. The basic result, confirmed by diffraction studies, is that the oxygen of the CO is displaced considerably from the heme normal (6, 7), in contrast to the situation in unhindered model compounds (8–10). A complication is that the CO bound to the protein occurs in several conformations. IR spectroscopy is especially useful in this case because even small populations of conformers, which may be difficult to detect by x-ray crystallography, can be discerned and characterized (11, 12). Because several conformers are present, the notions of a single binding constant or simple binding kinetics are not well defined. In fact, it has been known for many years that the rebinding step to the heme iron at low temperature is not given by a simple exponential rate constant but appears to be distributed (13). Some of the dispersion in the rate results from rebinding of the separate conformers as can be seen by monitoring the kinetics for individual conformers directly in the IR (12, 14).

With the advent of site-specific mutants of Mb and Hb, it has become possible to engineer changes in the interaction between the protein and ligands. Extensive measurements of the ligand rebinding kinetics in a wide range of human and sperm whale (SW) Mb mutants demonstrate enormous variations in both the geminate and bimolecular binding kinetics (15–19). Although trends can be discerned, it is often difficult to understand the effects in terms of specific interactions. We have measured the IR spectrum for a series of human Mb distal side mutants. Large effects are seen that can be quantitated and correlated with the observed ligand binding kinetics.

MATERIALS AND METHODS

The preparation and purification of recombinant human Mb and its mutants have been described elsewhere (15, 20–22). Mutations at His-64, Val-68, Lys-45, and Asp-60 (Fig. 1) were all based on a mutant of human Mb with the Cys-110 → Ala change; this mutant is used as our reference protein and is denoted wild type (WT). The mutant genes H64L and H64V were from M. Ikeda-Saito (Case Western Reserve University).

Concentrated stocks of the mutant Mbs were prepared; the buffer used for samples at pH >6 was 0.1 M sodium phosphate and for samples with pH <6 was 0.1 M citrate/borate/phosphate buffer (42). A calculated quantity of 95% (wt/vol) glycerol, similarly buffered, was then added to make the sample 75% glycerol. The samples were deoxygenated by stirring under a CO atmosphere and then reduced with sodium dithionite. The final concentration of MbCO was 1–3 mM. About 30 μl of the sample was withdrawn with a gas-tight syringe and injected into a 0.1-mm-path-length temperature-controlled cell with CaF_2 windows. Single-beam IR spectra were collected on a Perkin–Elmer 1600 series Fourier transform IR spectrophotometer with 2 or 4 cm^{-1} resolution at temperatures between 100 K and 300 K. Solvent spectra, collected at the same pH, glycerol concentration, and temperature, were used as a reference. The final spectrum was an average of 256, or in some cases, 1024 scans. Photolyzed spectra were obtained at 100 K with illumination

The publication costs of this article were defrayed in part by page charge payment. This article must therefore be hereby marked "*advertisement*" in accordance with 18 U.S.C. §1734 solely to indicate this fact.

Abbreviations: WT, wild type; SW, sperm whale; IR, infrared; Mb, myoglobin; Hb, hemoglobin.

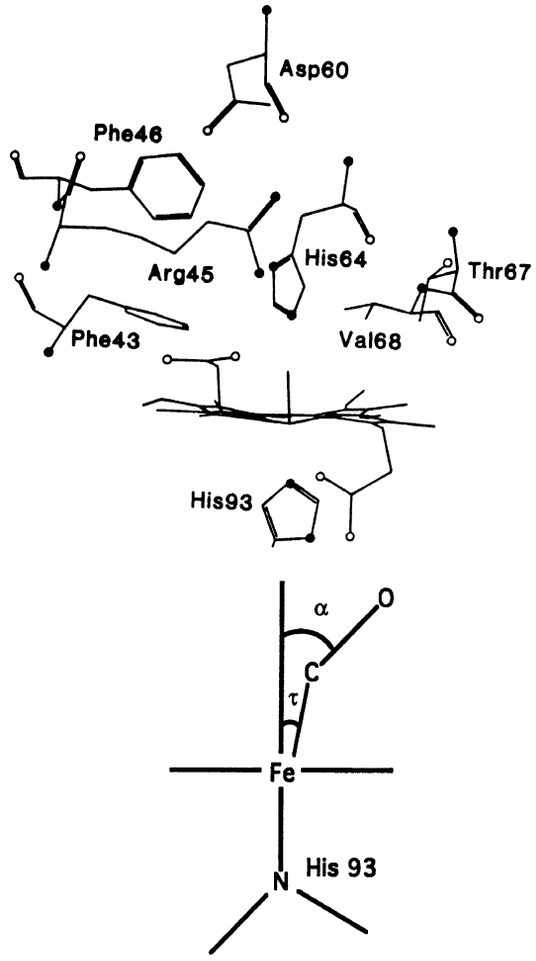

FIG. 1. (*Upper*) Stereochemistry of the residues surrounding the heme iron in the distal pocket of SW metMb (1). An essentially identical structure is observed for human Mb K45R (2). (*Lower*) The parameters defining the geometry of the bound CO are shown in an expanded view.

from a 300-W high-pressure Xe-arc lamp after passage through a water filter. Difference spectra (photolyzed minus unphotolyzed) were then obtained by subtracting the unphotolyzed spectrum at the same temperature. After each run the pH of the sample was measured directly with an Ingold microelectrode.

RESULTS

The CO stretch region of the IR spectrum of human WT MbCO at temperatures between 100 K and 300 K is shown in Fig. 2. At 300 K, two peaks are resolved, with frequencies of 1966 and 1945 cm^{-1}. Following the notation used for SW MbCO (12), the 1966 and 1945 cm^{-1} bands in WT are denoted A_0 and A_1, respectively. Decreasing the temperature produces the following changes in the spectrum: (*i*) the peak at 1945 cm^{-1} (A_1) shifts to higher frequency; (*ii*) the area of A_0 increases with respect to A_1, particularly at low pH; and (*iii*) the bandwidth of both peaks decreases (the A_1 peak is unusually broad at 300 K). The spectrum continues to change even below 220 K, which is near the glass transition temperature of the solvent. To ascertain that the sample was sufficiently equilibrated at each temperature, the temperature was lowered from above the glass transition to 170 K and held there for 20 min before recording the spectrum shown (this is the protocol normally used). The temperature was then lowered to 100 K, and the 100 K spectrum shown (which is different from the one at 170 K) was acquired. The sample was then warmed back up to 170 K and another spectrum was recorded. The two spectra at 170 K were found to be

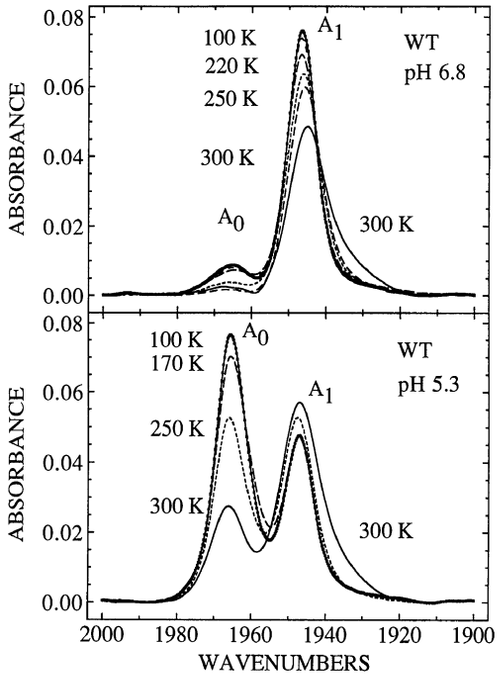

FIG. 2. IR absorption spectra of CO bound to human Mb WT in 75% glycerol buffer at pH 6.8 (*Upper*) and pH 5.3 (*Lower*). The peaks near 1965 cm^{-1} and 1945 cm^{-1} are labeled A_0 and A_1, following the notation used for the corresponding bands in SW MbCO (12). Some spectra at intermediate temperatures are omitted for clarity.

essentially identical; thus, the changes are reversible on the time scale of the experiment.

Spectra of the His-64 mutants as a function of temperature are shown in Fig. 3. H64V and H64L show only a single narrow band near 1970 cm^{-1} at all temperatures, with a bandwidth of 8.3 cm^{-1} at 100 K. H64A exhibits at least two resolved components, the relative areas of which vary with temperature. These two components are more closely spaced than in WT, with peaks near 1972 and 1966 cm^{-1}; thus the band corresponding to the A_1 conformer in WT is not seen under any conditions examined. The spectrum of H64Q at any temperature consists of a broad band but with unresolved structure. At 300 K, the peak is at 1945 cm^{-1}, which is the same as A_1 in WT, but the spectrum is much more temperature-dependent than WT at this pH (see Fig. 2).

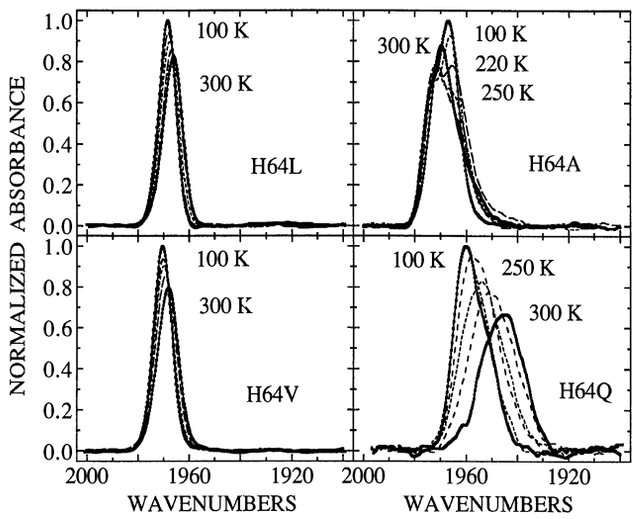

FIG. 3. IR absorption spectra of the bound CO in the distal His mutants H64L, H64V, H64A, and H64Q in 75% glycerol/phosphate, pH 6.8. The spectra for each mutant are normalized to the tallest peak at 100 K; the actual peak absorbances at 100 K were as follows: H64L, 0.038; H64V, 0.042; H64A, 0.018; H64Q, 0.009. For H64L and H64V, the spectra at 170 K overlap those at 100 K.

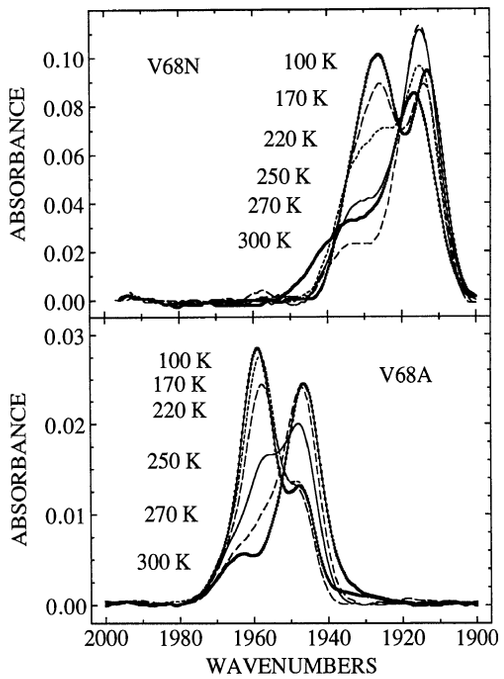

FIG. 4. IR absorption spectra for the mutants V68N (*Upper*) and V68A (*Lower*) in 75% glycerol/phosphate, pH 6.8. The spectra of V68N do not show any other distinguishable features below 1900 cm^{-1}.

The spectra of the Val-68 mutants are shown in Fig. 4. The spectrum of V68N at 300 K is greatly shifted with respect to WT, with a major peak at 1912 cm^{-1}; at low temperatures, however, the peak near 1928 cm^{-1} becomes larger. As in the hydrophobic His-64 mutants, the A_1 conformer of WT is not seen at any temperature. The spectrum of V68A at 300 K in Fig. 4 *Lower* displays two bands with peak frequencies of 1947 and 1963 cm^{-1} at 300 K, which are close to the peak frequencies in WT. But the area of the band at 1963 cm^{-1} relative to the 1947 cm^{-1} band is larger than in WT at 300 K. Furthermore, this band shifts much more with temperature than the A_0 band of WT. The intensity of this band increases with decreasing temperature, until it becomes the major band below about 250 K. The data shown in Figs. 2–4 are summarized in Table 1.

Steady-state difference spectra (photolyzed minus unphotolyzed; ΔA) at 100 K are displayed for WT MbCO and two mutants, H64A and V68N, in Fig. 5. The absolute absorbance spectra with and without illumination are also shown. Differential effects on individual conformers reflect differences in the rebinding kinetics for each conformer.†

DISCUSSION

Geometry of the Bound CO. The sensitivity of the IR spectrum of bound CO to the structure of the heme pocket is shown clearly in this work by the range of behavior exhibited by proteins containing single-amino acid substitutions in the distal pocket and by the changes with temperature and pH. There is a significant difference between SW MbCO and human MbCO: the 1930 cm^{-1} (A_3) peak of SW MbCO (12, 24) is not seen for the human protein under similar conditions.

Table 1. IR parameters for CO bound to human Mb mutants

	100 K			300 K		
Protein	ν, cm^{-1}	$\Delta\nu_{1/2}$, cm^{-1}	Relative area	ν, cm^{-1}	$\Delta\nu_{1/2}$, cm^{-1}	Relative area
WT (pH 6.8)	1947	9.0	0.89	1945	10.6	0.83 (95)
	1965	ND	0.11	1967	ND	0.04 (5)
WT (pH 5.3)	1947	9.3	0.39	1947	13.3	0.62 (73)
	1966	10.0	0.61	1966	11.4	0.23 (27)
H64Q	1960	15.5	1.00	1945	21.1	1.00
H64L	1968	7.9	1.00	1966	9.0	0.97
H64V	1970	8.3	1.00	1968	10.0	0.95
H64A	1967	14.4	0.72	1970	12.5	1.00
	1973	ND	0.28			
V68A	1948	ND	0.28	1947	12.1	0.75 (85)
	1959	11.6	0.72	1963	ND	0.13 (15)
V68N	1915	13.0	0.48	1917	17.4	0.65 (71)
	1927	14.8	0.52	1933	ND	0.26 (29)

For proteins, buffer at pH 6.8 ± 0.1 was used unless otherwise indicated. The integrated areas of the bands are normalized to the total area at 100 K for each protein. The percentage of each conformer present at 300 K is shown in parentheses. ND, could not be accurately determined due to overlap.

This is quite revealing, as the x-ray structure of the met form of human K45R (2), which has a very similar IR spectrum (data not shown) to human WT (Fig. 2), is nearly identical to the SW protein (1). Likewise, the proton NMR chemical shifts of the heme pocket residues in human MbCO are also virtually identical to those in SW MbCO (17, 21, 25). Thus, the absence of the A_3 peak in human WT MbCO is probably due to a combined effect of slight shifts in the positions of these residues. This is supported by recent work on human Mb by other workers (26).

The analysis of CO vibrational spectra in terms of structure and bonding has benefited greatly from linear dichroism studies. That work demonstrates that the apparent angle α of the CO relative to the heme normal (shown in Fig. 1) in the conformers observed for SW Mb is in the inverse order of their peak frequencies (27, 28).‡ The opposite trend would be expected if the carbon of the CO was located directly above the iron, and the observed angle α measured only the bend of the Fe–C–O from linearity. This is because a reduction in the Fe–C–O angle (increase in α) should decrease Fe→π^* (CO) back bonding, strengthening the CO bond and thus increasing the peak frequency. The situation is more complex, however, as contributions from the tilt of the (His-93)N–Fe–C axis (the angle τ in Fig. 1 *Lower*) and from porphyrin buckling should decrease the CO stretch frequency (29). Li and Spiro (29) have shown that these distortions require less energy than to bend the Fe–C–O bond. This appears to be supported by studies on hindered model compounds where the Fe–C–O is close to linear, but increased hindrance is accompanied by increased tilting and ruffling of the porphyrin, which is associated with a lowered CO stretch frequency (30–32). Recent analyses of neutron diffraction data on SWMbCO (7) and x-ray diffraction data on HbCO (33) show that these distortions are also present in the proteins, and this may account for the observed inverse relationship between ν_{CO} and the observed angle α. There is a further functional correlation in the case of SW MbCO: a larger apparent angle

†It has generally been assumed that the oscillator strengths for different transitions in the IR corresponding to different CO conformers are identical. Thus, the relative areas under the IR peaks are taken to represent the relative populations of the conformers (11, 23). There is no evidence that the quantum yield for the photodissociation of different conformers is different; consequently, differences in the relative intensities of the IR bands during steady-state photolysis reflect differences in rebinding kinetics.

‡The interpretation of linear dichroism experiments in terms of the angle α between the CO bond direction and the heme normal tacitly assumes that the direction of the transition dipole moment for the IR band lies along the CO bond direction (27, 28). Because the CO interacts strongly with the Fe, this may not be entirely accurate. It is also assumed that the transition dipole moment of the Soret bands used to induce linear dichroism in the sample lies in the heme plane. To the extent that the porphyrin is ruffled in different conformations (29), this may not be precisely correct.

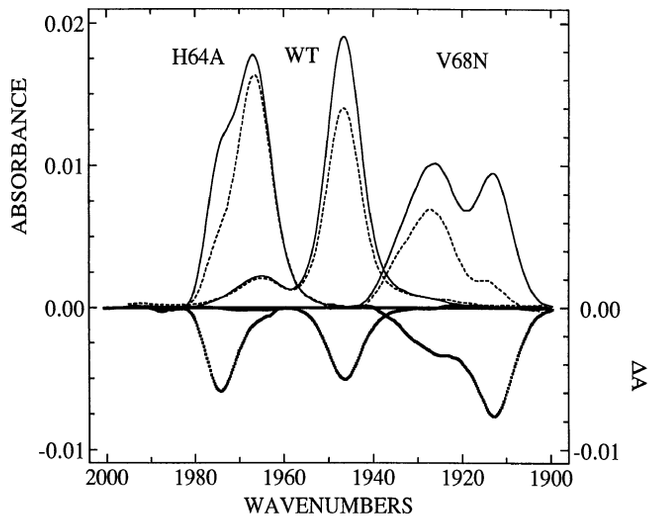

FIG. 5. Partial photolysis at 100 K (pH 6.8).† The unphotolyzed IR spectra of WT and two mutants are shown as solid lines. The dashed lines are the absolute absorbance spectra of these proteins under illumination, and the dotted lines are the corresponding difference spectra (photolyzed minus unphotolyzed).

α correlates with a larger CO rebinding barrier as measured by the kinetics of the individual IR conformers (12, 14). The absence of the slow rebinding A_3 conformer in human Mb may explain why CO rebinding to human Mb after flash photolysis (15, 16) is faster than for SW Mb (13).

Based on the correlations between ν_{CO} and the structure described above, it is likely that the single high-frequency conformer seen in H64V and H64L (Fig. 3) has a structure more similar to A_0 than A_1 or A_3. The higher ν_{CO} in these mutants suggests that the CO is even more parallel to the heme normal than in A_0. For H64A, there is also a low-temperature peak at $\approx$1967 cm^{-1}. A reasonable explanation is that this conformation in H64A is due to the presence of a water molecule near the entrance to the heme pocket (7). The single peak in H64V and H64L may be because of the exclusion of this water molecule by the bulkier hydrophobic side chains.

The IR spectra of H64Q show that the ν_{CO} is decreased to 1945 cm^{-1} at 300 K, similar to WT; but this band is much broader than the corresponding band in WT (linewidths, 23.2 and 10.6 cm^{-1}, respectively), and it is unusually temperature-dependent, shifting to 1960 cm^{-1} at 100 K, which is closer to the A_0 conformer in WT. The linewidth and the lack of well-resolved peaks in H64Q suggest that a larger range of conformations is accessible to the bound CO. The resolution into well-defined peaks in WT is, therefore, due to properties unique to the distal His, for example, its limited conformational space (4) and its pK_a (23, 34, 35).

Large perturbations of the IR spectrum are also seen for the Val-68 mutants (Fig. 4). This clearly demonstrates that residues other than the distal His can have a major effect on the bonding of CO. The Val-68 $\rightarrow$ Asn replacement results in an unprecedented shift of 30 cm^{-1} in the major conformer (from A_1 of WT) at 300 K; this is the lowest CO stretch frequency ever observed for any mutant of Mb or Hb (36). Interestingly, lowering the temperature increases the intensity of a band near 1930 cm^{-1}; such a temperature-dependent increase in a band about 15–20 cm^{-1} higher than the major band at 300 K is seen in all proteins containing a His at the distal position (WT, V68A, V68N, K45R, and D60E; for the last two, data not shown). Because the lowest frequency conformer in SW MbCO has the largest angle α, it is reasonable to suggest that the conformers of V68N are even more hindered. An additional possibility is a contribution due to direct electron donation from the Asn into the π^*-orbital of CO; however, we do not yet have direct information on this possibility.

Connection Between IR Spectra and Rebinding Kinetics. The kinetics of CO rebinding to these proteins have been studied as a function of temperature, and rebinding barrier heights for the final step at iron have been obtained in the temperature range of 250–300 K; details of the analysis are presented elsewhere (17, 18). The key result relevant to the Fourier transform IR data is that the final rebinding barrier heights for these mutants are in the order V68A $\approx$ H64L < H64V $\approx$ H64A < WT < V68N. Comparison of the IR spectra of the mutants (Table 1) with these trends in the final barrier heights for CO recombination shows that all the proteins that have higher frequency conformers than WT (in the same temperature range) also have smaller rebinding barriers. Conversely, V68N, which has lower frequency conformers than WT, has a larger rebinding barrier height. As a lower CO stretch frequency is associated with a more hindered conformation of the bound CO, a larger barrier at the final step of the binding is likely due to greater steric hindrance from distal residues. H64A, even though it has the highest frequency conformer of all, also has a significant population of a lower-frequency conformer in the temperature range of the kinetics measurement and, thus, has an apparent intermediate barrier height. V68A, with an increased population of a high-frequency conformer, has a smaller rebinding barrier height than WT. It is somewhat surprising that it has lower barrier heights than the hydrophobic H-64 mutants; in fact, its rebinding barrier height as well as its overall kinetics are quite similar to H64L, indicating that the structure of the bound CO may be similar. The difference in peak frequency between the two proteins ($\approx$6 cm^{-1}) may be a measure of the decrease in ν_{CO} due to the presence of the distal His (35, 37).

The results of partial (steady state) photolysis experiments at 100 K (Fig. 5), when no ligands escape from the pocket, corroborate the above conclusions but also raise several issues. (*i*) By comparison with the intensities of the unphotolyzed sample, it is observed that different IR bands exhibit a different extent of photolysis, showing that the rebinding rates of different conformers at 100 K can vary widely even within a given protein.† (*ii*) For roughly the same light intensity, a much higher proportion of the total population is photolyzed for V68N than for the others.† This suggests that the rebinding rate decreases with ν_{CO}. Further, for both WT and V68N, it is observed that the area of the lower frequency band decreases more on illumination. However, for H64A, the rates are reversed; the lower frequency conformer apparently rebinds with a rate much faster than the higher frequency one. This may be explained by the fact that the correlation of the IR frequency is with the barrier height, as this is where steric contributions from the protein are expected, and not with the rebinding rate, which depends on the prefactor as well. It may be that the lower frequency conformer of H64A has a more restricted pocket in the geminate state than the higher frequency one, leading to a larger prefactor. Thus, the temperature dependence is essential in attempting to correlate the IR bands to the kinetics.

Comparisons with Other Proteins. Limited IR data has been published for other Mb and Hb mutants, and some comparisons can be made. The IR spectrum of the mutant H64G in SW Mb at 10 K is unusually broad and peaks at 1973 cm^{-1} (38). For human Mb H64A, two closely spaced peaks are observed (Fig. 2). Thus, a reasonable suggestion is that two conformers are also present in SW H64G, but they are less well resolved. The rebinding barrier height for SW H64G below 160 K was found to be smaller than for native SW MbCO, which is in agreement with our results for human Mb H64A. Recently, a study of Leu-29 mutants in human Mb showed an increase in a low-frequency IR peak, and the bimolecular CO rebinding of these mutants was found to be

slower than WT (26), which is consistent with our results (geminate rebinding has not yet been reported). The IR spectrum of a bovine Mb mutant, H64R, exhibits a single band at 1957 cm^{-1} at room temperature in Tris buffer (pH 8.5) (39), but the rebinding kinetics have not been reported. A rough comparison can be made with the β chain of Hb Zurich, which also contains the distal His → Arg mutation; in this case, a study of the rebinding kinetics below 200 K indicated that the barrier was indeed smaller than in the corresponding HbA β chains (40, 41), consistent with the trends we are seeing.

We thank Professor Ikeda-Saito for the mutant genes H64L and H64V. This work was supported, in part, by a grant from the National Institutes of Health (GM-27738).

1. Takano, T. (1977) *J. Mol. Biol.* **110,** 569–584.
2. Hubbard, S. R., Hendrikson, W. A., Lambright, D. G. & Boxer, S. G. (1990) *J. Mol. Biol.* **213,** 215–218.
3. Stryer, L. (1988) *Biochemistry* (Freeman, New York).
4. Makinen, M. W., Houtchens, R. A. & Caughey, W. S. (1979) *Proc. Natl. Acad. Sci. USA* **76,** 6042–6046.
5. Alben, J., Beece, D., Bowne, S. F., Doster, W., Eisenstein, L., Frauenfelder, H., Goode, D., McDonald, J., Marden, M., Moh, P., Reinisch, L., Reynolds, A., Shyamsunder, E. & Yue, K. T. (1982) *Proc. Natl. Acad. Sci. USA* **79,** 3744–3748.
6. Kuriyan, J., Wilz, S., Karplus, M. & Petsko, G. A. (1986) *J. Mol. Biol.* **192,** 133–154.
7. Cheng, X. & Schoenborn, B. P. (1991) *J. Mol. Biol.* **220,** 381–399.
8. Peng, S.-M. & Ibers, J. A. (1976) *J. Am. Chem. Soc.* **98,** 8032–8066.
9. Collman, J. P., Brauman, J. I., Halbert, T. R. & Suslick, K. S. (1976) *Proc. Natl. Acad. Sci. USA* **73,** 3333–3337.
10. Collman, J. P., Brauman, J. I. & Doxsee, K. M. (1979) *Proc. Natl. Acad. Sci. USA* **76,** 6035–6039.
11. Shimada, H. & Caughey, W. S. (1982) *J. Biol. Chem.* **257,** 11893–11900.
12. Ansari, A., Berendzen, J., Brauenstein, D., Cowen, B. R., Frauenfelder, H., Hong, M. K., Iben, I. E. T., Johnson, B. J., Ormos, P., Sauke, T. B., Schulte, A., Steinbach, P. J., Vittitow, J. & Young, R. D. (1987) *Biophys. Chem.* **26,** 337–355.
13. Austin, R. H., Beeson, K. W., Eisenstein, L., Frauenfelder, H. & Gunsalus, I. C. (1975) *Biochemistry* **14,** 5355–5373.
14. Young, R. D., Frauenfelder, H., Johnson, J. B., Lamb, D. C., Nienhaus, G. U., Philipp, R. & Scholl, R. (1991) *Chem. Phys.* **158,** 315–327.
15. Lambright, D. G., Balasubramanian, S. & Boxer, S. G. (1989) *J. Mol. Biol.* **207,** 289–299.
16. Lambright, D. G., Balasubramanian, S. & Boxer, S. G. (1991) *Chem. Phys.* **158,** 249–260.
17. Lambright, D. G. (1992) Dissertation (Stanford Univ., Stanford).
18. Balasubramanian, S., Lambright, D. G., Marden, M. C. & Boxer, S. G. (1993) *Biochemistry* **32,** 2202–2212.
19. Carver, T. E., Olson, J. S., Smerdon, S. J., Krzywda, S., Wilkinson, A. J., Gibson, Q. H., Blackmore, R. S., Ropp, J. D. & Sligar, S. G. (1991) *Biochemistry* **30,** 4697–4705.
20. Varadarajan, R., Szabo, A. & Boxer, S. G. (1985) *Proc. Natl. Acad. Sci. USA* **82,** 5681–5684.
21. Varadarajan, R., Lambright, D. G. & Boxer, S. G. (1989) *Biochemistry* **28,** 3771–3781.
22. Ikeda-Saito, M., Lutz, R. S., Shelley, D. A., McKelvey, E. J., Mattera, R. & Hori, H. (1991) *J. Biol. Chem.* **266,** 23641–23647.
23. Morikis, D., Champion, P. M., Springer, B. A. & Sligar, S. G. (1989) *Biochemistry* **28,** 4791–4800.
24. Chance, M. R., Campbell, B. F., Hoover, R. & Friedman, J. M. (1987) *J. Biol. Chem.* **262,** 6959–6961.
25. Dalvit, C. & Wright, P. E. (1987) *J. Mol. Biol.* **194,** 313–327.
26. Adachi, S., Sunohara, N., Ishimori, K. & Morishima, I. (1992) *J. Biol. Chem.* **267,** 12614–12621.
27. Moore, J. N., Hansen, P. A. & Hochstrasser, R. M. (1988) *Proc. Natl. Acad. Sci. USA* **85,** 5062–5066.
28. Ormos, P., Braunstein, D., Frauenfelder, H., Hong, M. K., Lin, S. L., Sauke, T. B. & Young, R. D. (1988) *Proc. Natl. Acad. Sci. USA* **85,** 8492–8496.
29. Li, X.-Y. & Spiro, T. (1988) *J. Am. Chem. Soc.* **110,** 6024–6033.
30. Yu, N.-T., Kerr, E. A., Ward, B. & Chang, C. K. (1983) *Biochemistry* **22,** 4534–4540.
31. Kim, K., Fettinger, J., Sessler, J. L., Cyr, M., Hugdahl, J., Collman, J. P. & Ibers, J. A. (1989) *J. Am. Chem. Soc.* **111,** 403–405.
32. Cartier, C., Momenteau, M., Dartyge, E., Fontaine, A., Tourillon, G., Bianconi, A. & Verdaguer, M. (1992) *Biochim. Biophys. Acta* **1119,** 169–174.
33. Derewenda, Z., Dodson, G., Emsley, P., Harris, D., Nagai, N., Perutz, M. & Reynaud, J.-P. (1990) *J. Mol. Biol.* **211,** 515–519.
34. Ramsden, J. & Spiro, T. G. (1989) *Biochemistry* **28,** 3125–3128.
35. Fuchsman, W. H. & Appleby, C. A. (1979) *Biochemistry* **18,** 1309–1321.
36. Nagai, M., Yoneyama, Y. & Kitagawa, T. (1991) *Biochemistry* **30,** 6495–6503.
37. Lin, S. H., Yu, N.-T., Tame, J., Shih, D., Renaud, J. P., Pagnier, J. & Nagai, K. (1990) *Biochemistry* **29,** 5562–5566.
38. Braunstein, D., Ansari, A., Berendzen, J., Cowen, B. R., Egeberg, K. D., Frauenfelder, H., Hong, M. K., Ormos, P., Sauke, T. B., Scholl, R., Schulte, A., Sligar, S. G., Springer, B. A., Steinbach, P. J. & Young, R. D. (1988) *Proc. Natl. Acad. Sci. USA* **85,** 8497–8501.
39. Shimada, H., Dong, A., Matsushima, H. Y., Ishimura, Y. & Caughey, W. S. (1989) *Biochem. Biophys. Res. Commun.* **158,** 110–114.
40. Dlott, D. D., Frauenfelder, H., Langer, P., Roder, H. & Iorio, E. E. (1983) *Proc. Natl. Acad. Sci. USA* **80,** 6239–6243.
41. Steinbach, P. J., Ansari, A., Berendzen, J., Braunstein, D., Chu, K., Cowen, B. R., Ehrenstein, D., Frauenfelder, H., Johnson, J. B., Lamb, D. C., Luck, S., Mourant, J. R., Nienhaus, G. U., Ormos, P., Philipp, R., Xie, A. & Young, R. D. (1991) *Biochemistry* **30,** 3988–4001.
42. Sober, H. A., ed. (1970) *Handbook of Biochemistry* (CRC, Boca Raton, FL), 2nd Ed., pp. J-234.